

Supporting Information

MXene-Supported Single Atom Catalyst Selectively Converts CO₂ into Methanol and Methane†

*Hasan Al-Mahayni^a, Rongyu Yuan^a, Ali Seifitokaldani *^a*

^a Department of Chemical Engineering, McGill University, Montreal, Quebec, Canada. H3A 0C5

* Corresponding author: ali.seifitokaldani@mcgill.ca

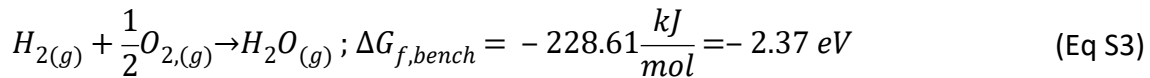
Computational details:

To compute energy differences of elementary proton coupled electron transfer (PCET) steps, the computational hydrogen electrode (CHE) model was used ¹:



$$E_{H^+ + e^-} = \frac{E_{H_{2(g)}}}{2}, \text{ @pH=0 and 1 atm} \quad (\text{Eq S2})$$

To calculate the formations energy from Eq (1) of the manuscript, the energy of Oxygen (O) must be calculated. Using the DFT energy of O₂ and dividing by 2 to obtain the energy of O has been shown to be inaccurate². Thus, we use the benchmarked Gibbs formation energy³ of H₂O_(g) to back-calculate the energy of O. The equations below were used:



$$E_{O,correction} = 0.57 \text{ eV} \quad (\text{Eq S4})$$

To obtain the correction energy for the oxygen atom, we calculate (from DFT simulations) the Gibbs formation energy of the reaction in Eq S3, which was $\Delta G_{f,sim} = -2.94 \text{ eV}$. We then take the simulated $\Delta G_{f,sim}$ and subtract $\Delta G_{f,bench}$ to get the correction energy.

To convert DFT energies to Gibbs free energy, the ASE thermochemistry module was used ⁴. Specifically, the Gibbs free energy of adsorbed intermediates and liquid products were approximated using the harmonic module, while gaseous reactants and products were

approximated using the ideal gas model at 1atm and room temperature (298.15 K). The equations for the harmonic model are below.

$$U(T) = E_{DFT} + E_{ZPE} + \sum_i^{harm\ DOF} \frac{\epsilon_i}{e^{\frac{-\epsilon_i}{k_B T}} - 1} \quad (\text{Eq S5})$$

$$S = k_B \sum_i^{harm\ DOF} \left[\frac{\epsilon_i}{e^{\frac{-\epsilon_i}{k_B T}} - 1} - \ln \left(1 - e^{\frac{-\epsilon_i}{k_B T}} \right) \right] \quad (\text{Eq S6})$$

$$G(T) = U(T) - TS(T) \quad (\text{Eq S7})$$

The equations for the ideal gas model are below:

$$H(T) = E_{DFT} + E_{ZPE} + \int_0^T Cp \, dT \quad (\text{Eq S8})$$

$$Cp = k_B + C_{V,trans} + C_{V,rot} + C_{V,vib} + C_{v,elec} \quad (\text{Eq S9})$$

$$S(T,P) = S_{trans} + S_{rot} + S_{elec} + S_{vib} - k_B \ln \left(\frac{P}{P^0} \right) \quad (\text{Eq S10})$$

$$G(T,P) = H(T) - TS(T,P) \quad (\text{Eq S11})$$

To calculate reaction energy differences from a PCET step:



$$\Delta E_{DFT} = E_{{}^*COOH} - E_{{}^*CO_2} - \frac{E_{H_2}}{2} \quad (\text{Eq S13})$$

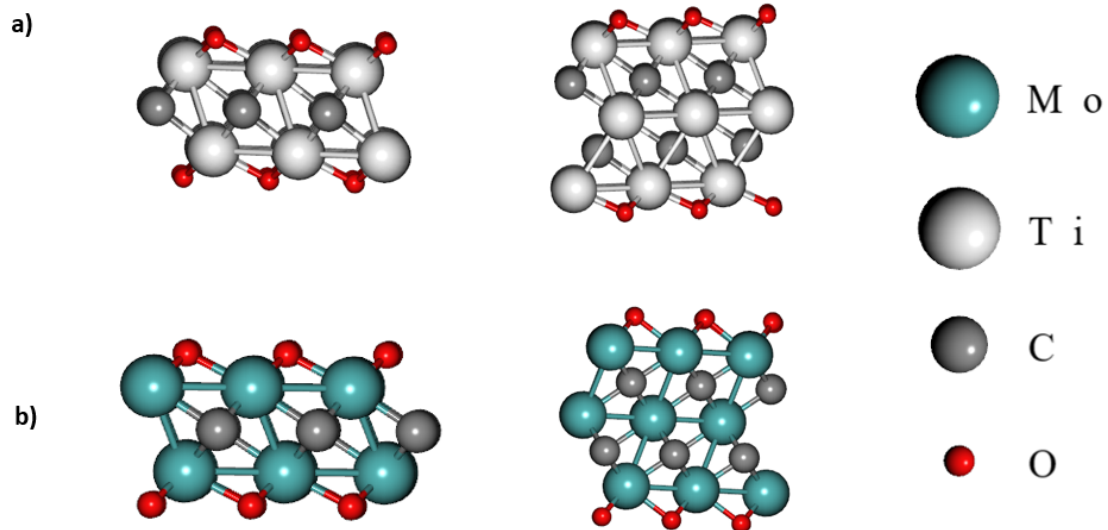


Figure S1. Four MXene supports that are used in this paper. (a) left: $\text{Ti}_{18}\text{C}_9\text{O}_{18}$; right: $\text{Ti}_{27}\text{C}_{18}\text{O}_{18}$.
 (b) left: $\text{Mo}_{18}\text{C}_9\text{O}_{18}$; right: $\text{Mo}_{27}\text{C}_{18}\text{O}_{18}$.

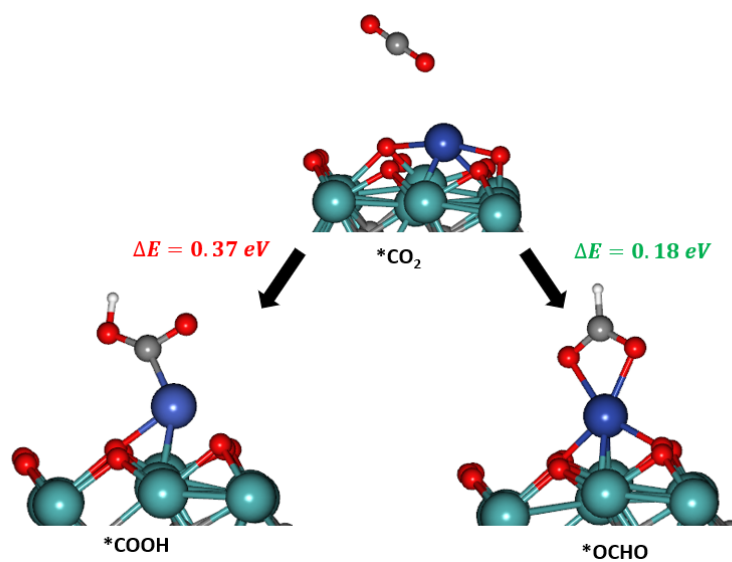


Figure S2. CO_2 protonation to OCHO or COOH on $\text{Ru}@\text{Mo}_2$ catalyst

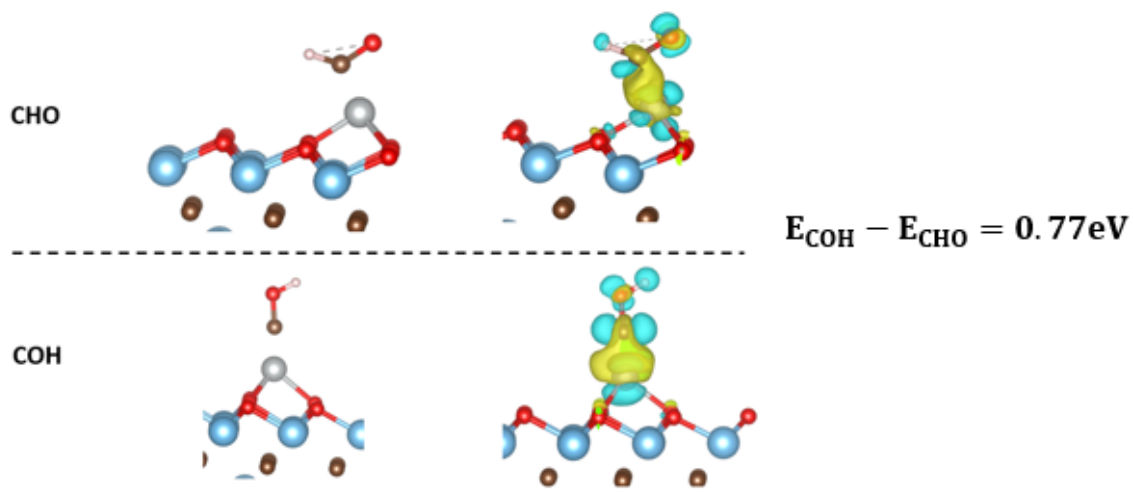


Figure S3. Charge delocalization of $^*\text{CHO}$ and $^*\text{COH}$ on Ni@Ti3. Blue color indicates areas where electrons are lost whereas yellow color indicates the opposite.

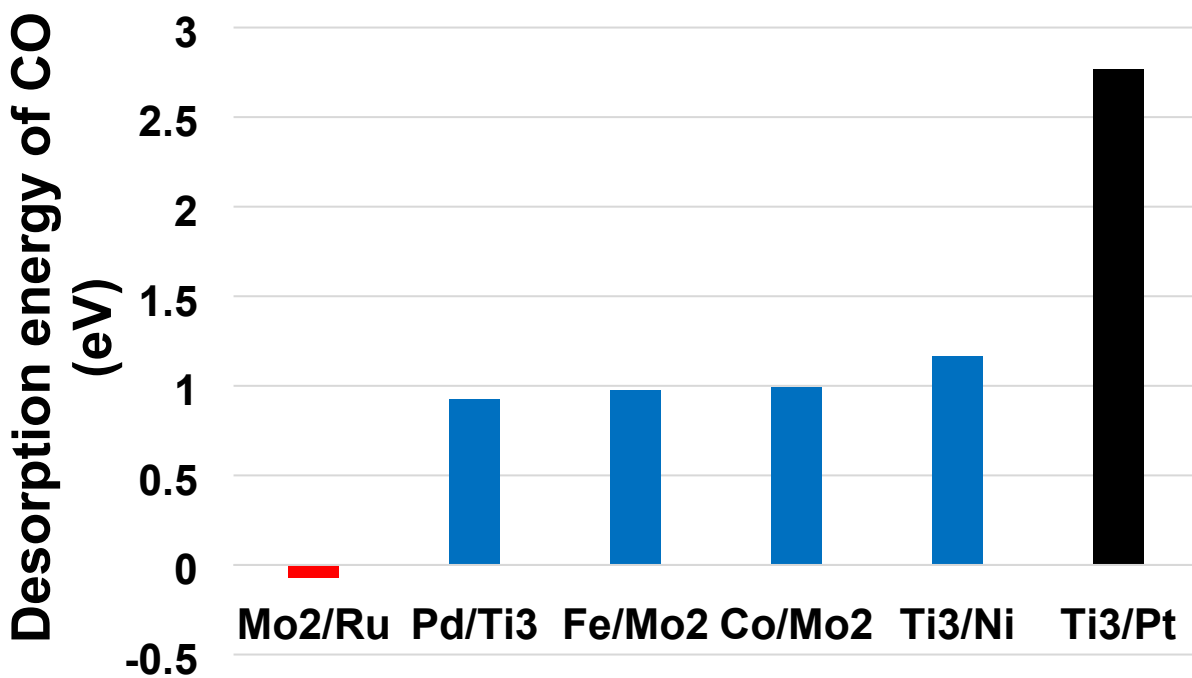


Figure S4. CO desorption energy (in Gibbs free energy) of the six selected catalysts.

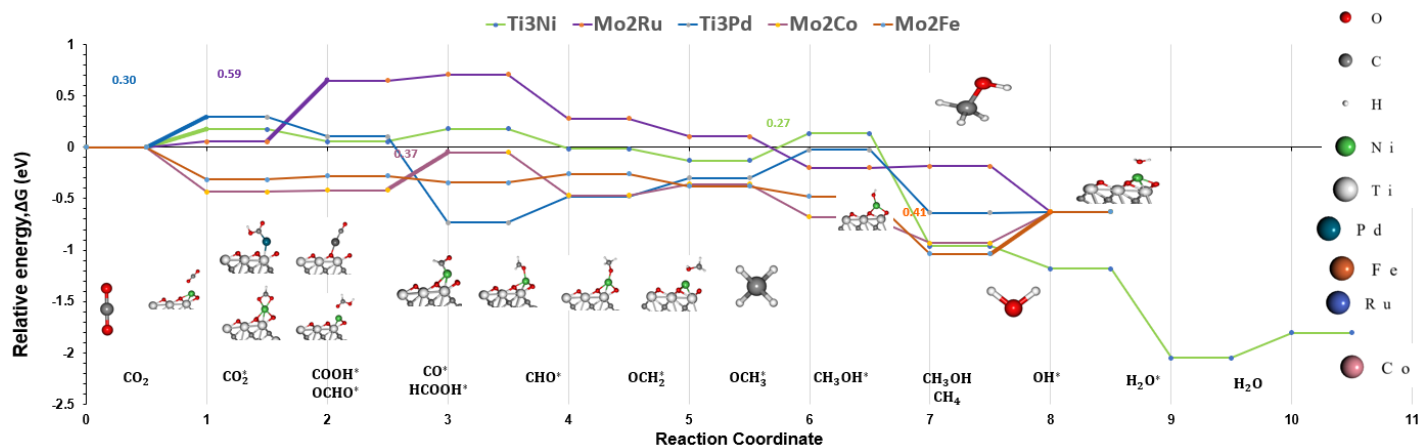


Figure S5. Energy diagram of the five final catalysts.

Table S1. Results comparing the HER and CO₂RR.

structure	CO2*	OCHO*	HCOOH*	CHO*	OCH2*	OCH3*	CH3OH	RDS	RDS-barrier	H*	Conclusion
Ti2/Co	-0.417	-0.878	0.272	-0.197	-0.080	-0.691	0.513	Ti2-Co-CH3OH	0.513	-0.238	Co@Mo2 Better
Ti2/Cu	-0.492	-0.217	-0.453	0.946	-1.195	-0.322	0.255	Ti2-Cu-CHO	0.946	-0.032	HER, High RDS barrier
Ti2/Fe	-0.390	-1.357	0.497	-0.073	-0.343	-0.890	1.078	Ti2-Fe-CH3OH	1.078	-0.412	HER, High RDS barrier
Ti2/Pt	-0.619	-0.881	-0.404	0.193	-0.378	-0.193	0.803	Ti2-Pt-CH3OH	0.803	-0.880	HER, High RDS barrier
Ti2/Ru	-0.280	-1.607	0.356	-0.059	-0.666	-0.203	0.983	Ti2-Ru-CH3OH	0.983	-0.893	HER, High RDS barrier
Ti2/Ni	-0.331	-0.249	-0.380	0.600	-0.656	-0.087	-0.375	Ti2-Ni-CHO	0.600	0.540	Ni@Ti2 better
Ti3/Co	-0.775	-0.852	0.158	-0.084	-0.191	-0.564	0.830	Ti3-Co-CH3OH	0.830	-0.574	High RDS barrier
Ti3/Cu	-0.893	0.008	-0.755	1.124	-1.331	-0.027	0.394	Ti3-Cu-CHO	1.124	0.118	Other Cu is better
Ti3/Fe	-0.733	-1.371	0.297	0.154	-0.405	-0.735	1.315	Ti3-Fe-CH3OH	1.315	-0.692	High RDS barrier
Ti3/Pt	-1.508	-0.362	-0.165	-0.047	0.079	-0.125	0.650	Ti3-Pt-CH3OH	0.650	-1.155	Good
Ti3/Ru	-0.581	-1.693	0.292	0.048	-0.099	-0.766	1.321	Ti3-Ru-CH3OH	1.321	-1.172	High RDS barrier
Ti3/Ni	-0.318	-0.463	-0.217	0.352	-0.424	-0.077	-0.331	Ti3-Ni-CHO	0.352	0.468	Good
Mo2/Co	-0.920	-0.317	0.024	0.147	-0.263	-0.636	0.487	Mo2-Co-CH3OH	0.487	0.019	High RDS barrier
Mo2/Cu	-0.138	-0.385	-0.729	1.197	-1.183	-0.163	-0.077	Mo2-Cu-CHO	1.197	0.462	Good
Mo2/Fe	-0.811	-0.218	-0.477	0.569	-0.386	-0.460	0.305	Mo2-Fe-CHO	0.569	0.174	High RDS barrier
Mo2/Pt	-1.385	-0.059	-0.925	0.785	-0.964	-0.506	1.576	Mo2-Pt-CH3OH	1.576	-0.684	Good
Mo2/Ru	-0.357	0.186	-0.201	-0.015	-0.473	-0.645	0.028	Mo2-Ru-OCHO	0.186	0.862	Ni@Ti3 better
Mo2/Ni	-0.433	-0.524	-0.212	0.461	-0.627	-0.654	0.510	Mo2-Ni-CH3OH	0.510	0.458	CO2 ads
Mo3/Co	1.407	-1.524	-0.199	0.459	-0.433	-0.633	-0.555	Mo3-Co-CO2	1.407	1.233	High RDS barrier
Mo3/Cu	1.348	0.085	-1.237	1.488	-1.448	0.329	-2.044	Mo3-Cu-CHO	1.488	2.416	CO2 ads
Mo3/Fe	1.410	-1.822	-0.195	0.676	-0.724	-0.772	-0.050	Mo3-Fe-CO2	1.410	1.120	CO2 ads
Mo3/Pt	1.238	-1.300	-0.747	0.448	0.328	-0.433	-1.011	Mo3-Pt-CO2	1.238	0.650	CO2 ads
Mo3/Ru	1.543	-2.070	-0.163	0.277	-0.233	-0.793	-0.039	Mo3-Ru-CO2	1.543	0.612	High RDS barrier
Mo3/Ni	-0.417	-1.044	-0.529	0.535	-0.510	-0.346	0.833	Mo3-Ni-CH3OH	0.833	-0.358	High RDS barrier
Ti3/Ag	-0.283	0.360	-1.065	1.231	-0.937	0.016	-0.800	Ti3-Ag-CHO	1.230	0.536	High RDS barrier
Ti3/Pd	-0.222	-0.414	-0.669	0.177	-0.136	-0.065	-0.148	Ti3-Pd-CHO	0.177	0.067	Good

0.513 RDS

Unfavourable

Favourable, but other catalysts of the same Transition Metal are better

Favourable

Table S2. *OCHO vs *COOH formation.

Structure	*OCHO (eV)	*COOH (eV)	E(*OCHO) > E(*COOH)
Co/Ti ₂	-0.878	-0.401	FALSE
Cu/Ti ₂	-0.217	0.213	FALSE
Fe/Ti ₂	-1.357	-0.652	FALSE
Pt/Ti ₂	-0.881	-0.778	FALSE
Ru/Ti ₂	-1.607	-1.035	FALSE
Ni/Ti ₂	-0.249	0.222	FALSE
Co/Ti ₃	-0.852	-0.412	FALSE
Cu/Ti ₃	0.008	0.522	FALSE
Fe/Ti ₃	-1.371	-0.637	FALSE
Pt/Ti ₃	-0.362	-0.262	FALSE
Ru/Ti ₃	-1.692	-1.060	FALSE
Ni/Ti ₃	-0.463	-0.460	FALSE
Co/Mo ₂	-0.317	0.206	FALSE
Cu/Mo ₂	-0.385	0.338	FALSE
Fe/Mo ₂	-0.218	0.236	FALSE
Pt/Mo ₂	-0.0593	0.0645	FALSE
Ru/Mo ₂	0.185	0.367	FALSE
Ni/Mo ₂	-0.524	0.168	FALSE
Co/Mo ₃	-1.523	¹	
Cu/Mo ₃	0.0851	0.581	FALSE
Fe/Mo ₃	-1.822		
Pt/Mo ₃	-1.300		
Ru/Mo ₃	-2.070		
Ni/Mo ₃	-1.044	1.165	FALSE

¹ There are blank slots for catalysts that were screened out early due to high adsorption energy of CO₂, making them unfavourable regardless of further steps.

Table S3. HCOOH desorption versus protonation to form *CHO.

Structure	E ₁ (HCOOH* to HCOOH) (eV)	E ₂ (HCOOH* to CHO*) (eV)	E ₂ >E ₁
Co/Ti ₂	1.013	-0.197	FALSE
Cu/Ti ₂	1.152	0.946	FALSE
Fe/Ti ₂	1.240	-0.073	FALSE
Pt/Ti ₂	1.894	0.193	FALSE
Ru/Ti ₂	1.522	-0.059	FALSE
Ni/Ti ₂	0.950	0.599	FALSE
Co/Ti ₃	1.460	-0.084	FALSE
Cu/Ti ₃	1.623	1.124	FALSE
Fe/Ti ₃	1.797	0.154	FALSE
Pt/Ti ₃	2.025	-0.047	FALSE
Ru/Ti ₃	1.972	0.048	FALSE
Ni/Ti ₃	0.988	0.352	FALSE
Co/Mo ₂	1.203	0.147	FALSE
Cu/Mo ₂	1.242	1.197	FALSE
Fe/Mo ₂	1.496	0.569	FALSE
Pt/Mo ₂	2.359	0.785	FALSE
Ru/Mo ₂	0.362	-0.015	FALSE
Ni/Mo ₂	1.158	0.461	FALSE
Co/Mo ₃	0.305	0.459	TRUE
Cu/Mo ₃	-0.207	1.487	TRUE
Fe/Mo ₃	0.597	0.676	TRUE
Pt/Mo ₃	0.800	0.449	FALSE
Ru/Mo ₃	0.680	0.277	FALSE
Ni/Mo ₃	1.980	0.535	FALSE

Table S4. *CHOH pathway vs *OCH₂ pathway.

Structure	E (*CHO to *CHOH) (eV)	E (*CHOH to *CH ₂ OH) (eV)	E (*CH ₂ OH to *CH ₃ OH) (eV)	RDS	Energy of RDS (eV)
Co/Ti₂	0.234	-1.143	0.651	Ti ₂ -Co-CH ₃ OH	0.513
Cu/Ti₂	-0.356	-0.674	-0.233	Ti ₂ -Cu-CHO	0.946
Fe/Ti₂	-0.047	-0.976	0.868	Ti ₂ -Fe-CH ₃ OH	0.868
Pt/Ti₂	-0.256	-0.581	1.069	Ti ₂ -Pt-CH ₃ OH	0.803
Ru/Ti₂	-0.189	-0.723	1.025	Ti ₂ -Ru-CH ₃ OH	0.983
Ni/Ti₂	-0.215	-0.837	-0.065	Ti ₂ -Ni-CHO	0.600
Co/Ti₃	0.052	-1.017	1.040	Ti ₃ -Co-CH ₃ OH	0.830
Cu/Ti₃	-0.480	-0.534	0.051	Ti ₃ -Cu-CHO	1.124
Fe/Ti₃	-0.094	-0.968	1.237	Ti ₃ -Fe-CH ₃ OH	1.237
Pt/Ti₃	-0.377	-0.494	1.475	Pt@Ti ₃ -CH ₃ OH	0.650
Ru/Ti₃	-0.171	-0.789	1.416	Ti ₃ -Ru-CH ₃ OH	1.321
Ni/Ti₃	-0.121	-1.404	0.693	Ni@Ti ₃ -CHO	0.352
Co/Mo₂	-0.098	-1.105	0.791	Co@Mo ₂ -CH ₃ OH	0.487
Cu/Mo₂	-0.864	-0.043	-0.516	Mo ₂ -Cu-CHO	1.197
Fe/Mo₂	0.032	-0.909	0.336	Fe@Mo ₂ -CHO	0.569
Pt/Mo₂	-1.604	0.619	1.091	Mo ₂ -Pt-CH ₃ OH	1.091
Ru/Mo₂	-0.243	-0.915	0.068	Ru@Mo ₂ -OCHO	0.186
Ni/Mo₂	-0.273	-1.028	0.530	Mo ₂ -Ni-CH ₃ OH	0.510
Co/Mo₃	²			Mo ₃ -Co-CO ₂	
Cu/Mo₃				Mo ₃ -Cu-CHO	
Fe/Mo₃				Mo ₃ -Fe-CO ₂	
Pt/Mo₃				Mo ₃ -Pt-CO ₂	
Ru/Mo₃				Mo ₃ -Ru-CO ₂	
Ni/Mo₃	0.067	0.690	-0.779	Mo ₃ -Ni-CH ₂ OH	0.690

² There are blank slots for catalysts that were screened out early due to high adsorption energy of CO₂, making them unfavorable regardless of further steps.

Table S5. DFT energy and Gibbs free energy data (eV). E_DFT is the DFT energy calculated at the ground state. E_ZPE is the zero-point energy as presented on Eq S3. Cv_harm is the harmonic heat capacity as defined in Eq S7. The TS term represents the temperature (298K) times the entropy. G is the Gibbs free energy (eV) as presented in Eq S9.

	E_DFT	E_ZPE	Cv_harm	TS	G	Extra G term
Ni@Ti ₃ -H ₂	-58102.57	0.123	0	0	-58102.44	0.123
Ni@Ti ₃ -CO ₂	-59115.76	0.378	0.078	-0.133	-59115.44	0.323
Ni@Ti ₃ -OCHO	-59132.03	0.673	0.073	-0.123	-59131.41	0.623
Ni@Ti ₃ -HCOOH	-59148.06	0.987	0.09	-0.156	-59147.14	0.921
Ni@Ti ₃ -CHO	-58694.95	0.498	0.067	-0.121	-58694.51	0.443
Ni@Ti ₃ -OCH ₂	-58711.18	0.785	0.074	-0.153	-58710.48	0.706
Ni@Ti ₃ -OCH ₃	-58727.07	1.102	0.078	-0.176	-58726.06	1.005
Ni@Ti ₃ -CH ₃ OH	-58744.40	1.457		-0.151	-58743.02	1.388
Ni@Ti ₃ -COOH	-59131.73	0.68	0.072	-0.113	-59131.09	0.64
Ni@Ti ₃ -CHOH	-58710.88	0.84	0.066	-0.111	-58710.08	0.795
Ni@Ti ₃ -COH	-58694.17					
Ni@Ti ₃ -CH ₂	-58273.76	0.606	0.024	-0.036	-58273.168	0.594
Ni@Ti ₃ -CH ₃	-58291.09	0.918	0.039	-0.078	-58290.211	0.88
Ni@Ti ₃ -O	-58522.06	0.08	0.029	-0.049	-58522.002	0.061
Ni@Ti ₃ -OH	-58540.24	0.364	0.044	-0.071	-58539.906	0.336
Ni@Ti ₃ -H ₂ O	-58557.48	0.685	0.067	-0.12	-58556.846	0.631
Ni@Ti ₃ -CO	-58679.81	0.232	0.052	-0.083	-58679.614	0.201
Ni@Ti ₃ -CH ₄	-58308.25	1.211	0.069	-0.147	-58307.119	1.132
Pt@Ti ₃ -H ₂	-56766.71	0.225	0.008	-0.011	-56766.489	0.222
Pt@Ti ₃ -CO ₂	-57778.77	0.332	0.063	-0.114	-57778.495	0.281
Pt@Ti ₃ -OCHO	-57794.65	0.68	0.07	-0.117	-57794.016	0.633
Pt@Ti ₃ -HCOOH	-57810.92	0.953	0.061	-0.101	-57810.008	0.913
Pt@Ti ₃ -CHO	-57358.21	0.492	0.03	-0.048	-57357.739	0.474
Pt@Ti ₃ -OCH ₂	-57373.94	0.796	0.044	-0.072	-57373.175	0.767
Pt@Ti ₃ -OCH ₃	-57389.87	1.108	0.078	-0.156	-57388.847	1.029
Pt@Ti ₃ -CH ₃ OH	-57406.70	1.46	0.105	-0.228	-57405.37	1.336
Pt@Ti ₃ -COOH	-57794.84	0.639	0.052	-0.084	-57794.241	0.607
Pt@Ti ₃ -O	-57184.48	0.068	0.016	-0.027	-57184.43	0.057
Pt@Ti ₃ -OH	-57202.89	0.362		-0.046	-57202.55	0.343
Pt@Ti ₃ -H ₂ O	-57219.57	0.697		-0.117	-57218.931	0.642
Pt@Ti ₃ -CO	-57343.25	0.23	0.035	-0.059	-57343.041	0.206
Pt@Ti ₃ -CH ₄	-56970.83	1.194	0.091	-0.192	-56969.74	1.093

Pd@Ti3-CO2	-57971.23	0.393	0.07	-0.113	-57970.886	0.349
Pd@Ti3-OCHO	-57987.46	0.675		-0.12	-57986.831	0.626
Pd@Ti3-HCOOH	-58003.94	0.974	0.085	-0.142	-58003.02	0.915
Pd@Ti3-COOH	-57987.55	0.668	0.079	-0.128	-57986.932	0.618
Pd@Ti3-CO	-57535.13	0.226		-0.091	-57534.944	0.19
Pd@Ti3-CHO	-57551.00	0.51		-0.111	-57550.542	0.461
Pd@Ti3-OCH2	-57566.95	0.809			-57566.218	0.730
Pd@Ti3-OCH3	-57582.82	1.115	0.088	-0.179	-57581.798	1.024
Pd@Ti3-CH3OH	-57599.62	1.444			-57598.265	1.357
Pd@Ti3-CH4	-57163.84	1.212	0.09	-0.206	-57162.754	1.095
Pd@Ti3-O	-57377.40	0.079		-0.043	-57377.338	0.063
Pd@Ti3-H2	-56959.37				-56959.165	0.202
Pd@Ti3-OH	-57395.62	0.346	0.058	-0.124	-57395.335	0.280
Pd@Ti3-H2O	-57413.12	0.694	0.059	-0.097	-57412.465	0.655
Ru@Mo2-H2	-45274.55	0.224	0.005	-0.007	-45274.33	0.223
Ru@Co@Mo22	-46287.49	0.375	0.085	-0.214	-46287.24	0.246
Ru@Mo2-OCHO	-46303.11	0.635	0.047	-0.077	-46302.5	0.606
Ru@Mo2-HCOOH	-46319.12	0.934	0.105	-0.215	-46318.295	0.823
Ru@Mo2-CHO	-45866.38	0.495	0.026	-0.04	-45865.897	0.481
Ru@Mo2-OCH2	-45882.66	0.805	0.081	-0.155	-45881.928	0.732
Ru@Mo2-OCH3	-45899.11	1.124	0.091	-0.185	-45898.084	1.03
Ru@Mo2-CH3OH	-45915.27	1.452	0.105	-0.211	-45913.927	1.346
Ru@Co@Mo2OH	-46302.92	0.641	0.049	-0.075	-46302.312	0.615
Ru@Mo2-O	-45694.91	0.078	0.034	-0.064	-45694.869	0.048
Ru@Mo2-OH	-45712.15	0.362	0.045	-0.074	-45711.822	0.333
Mor-Ru-H2O	-45728.63	0.693	0.059	-0.097	-45727.983	0.654
Ru@Co@Mo2	-45850.24	0.222	0.057	-0.101	-45850.068	0.179
Ru@Mo2-CH4	-45479.75	1.25	0.106	-0.26	-45478.656	1.095
Co@Mo2-H2	-46656.02	0.21	0.008	-0.011	-46655.816	0.207
Co@Mo2-CO2	-47668.67	0.381	0.08	-0.145	-47668.359	0.316
Co@Mo2-OCHO	-47684.80	0.677	0.079	-0.148	-47684.194	0.607
Co@Mo2-HCOOH	-47700.58	0.955	0.064	-0.111	-47699.679	0.906
Co@Mo2-CHO	-47247.68	0.493	0.071	-0.154	-47247.274	0.409
Co@Mo2-OCH2	-47263.75	0.792	0.067	-0.124	-47263.02	0.734
Co@Mo2-OCH3	-47280.19	1.113	0.095	-0.199	-47279.191	1.008
Co@Mo2-CH3OH	-47296.69	1.463	0.081	-0.15	-47295.303	1.394
Co@Mo2-COOH	-47684.27	0.646	0.049	-0.078	-47683.661	0.616
Co@Mo2-O	-47075.43	0.07	0.036	-0.068	-47075.398	0.038
Co@Mo2-OH	-47093.36	0.38	0.038	-0.06	-47093.011	0.358
Co@Mo2-CO	-47231.96	0.24	0.048	-0.076	-47231.753	0.212

Co@Mo2-H2O	-47110.55	0.699	0.047	-0.073	-47109.878	0.672
Co@Mo2-CH4	-46860.98	1.269	0.094	-0.208	-46859.834	1.155
Fe@Mo2-H2	-46060.21	0.217	0.006	-0.008	-46060.004	0.214
Fe@Mo2-CO2	47072.91 7	0.392	0.078	-0.141	-47072.589	0.328
Fe@Mo2-OCHO	-47088.94	0.643	0.091	-0.196	-47088.406	0.538
Fe@Mo2-HCOOH	-47105.22	0.965	0.08	-0.141	-47104.325	0.904
Fe@Mo2-CHO	-46651.90	0.525	0.042	-0.075	-46651.414	0.490
Fe@Mo2-OCH2	-46668.10	0.782	0.073	-0.146	-46667.392	0.707
Fe@Mo2-OCH3	-46684.37	1.119	0.093	-0.188	-46683.346	1.022
Fe@Mo2-CH3OH	-46701.14	1.462	0.09	-0.17	-46699.759	1.382
Fe@Mo2-COOH	-47088.49	0.636	0.053	-0.096	-47087.897	0.593
Fe@Mo2-O	-46480.62	0.074	0.037	-0.076	-46480.584	0.035
Fe@Mo2-OH	-46498.04	0.361	0.027	-0.041	-46497.692	0.346
Fe@Mo2-CO	-46636.29	0.234	0.051	-0.082	-46636.086	0.203
Fe@Mo2-H2O	-46515.08	0.707	0.042	-0.063	-46514.394	0.684
Fe@Mo2-CH4	-46265.19	1.269	0.075	-0.164	-46264.014	1.180

Table S6. Key Gibbs free energy differences for drawing conclusions on product selectivity.

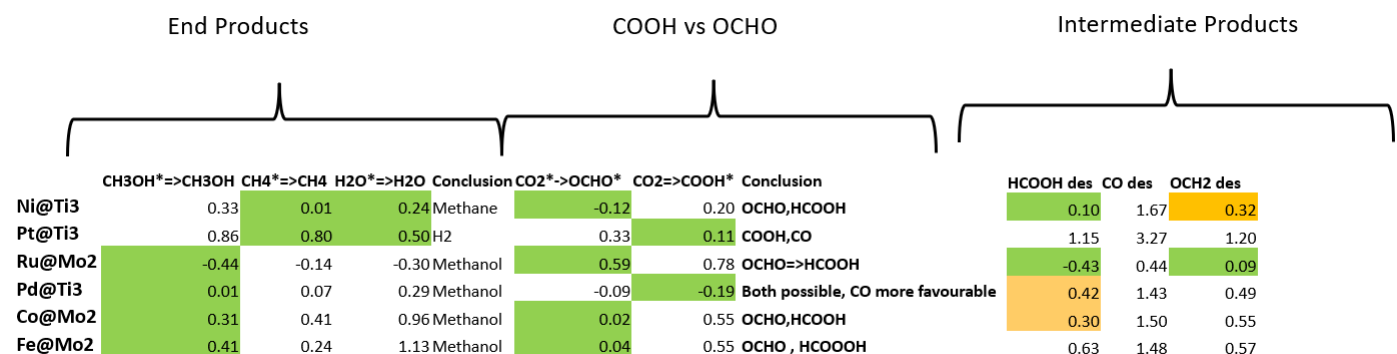


Table S7 Example of the six final catalysts that have been previously synthesized in experiments

Identified Catalysts	Structure synthesized	Applications
Ni @Ti ₃	NiO on Ti ₃ C ₂ [5] Ni SAC on O-terminated Ti ₃ C ₂ [6]	Supercapacitor Hydrazine oxidation
Pd @Ti ₃	Pd SAC on Nb ₂ CT ₂ (T= O, F, and OH) [7]	OER, ORR
Pt @ Ti ₃	Pt SAC on O-terminated Ti ₃ C ₂ [8,9]	CO ₂ functionalization, Aniline conversion, HER
Ru @ Mo ₂	Ru SAC on O-terminated Mo ₂ C [10,11]	Nitrogen Reduction Reaction, HER

Co @Mo₂	Co SAC on O-terminated Mo₂ ^[12]	OER and HER
Fe @Mo₂	Fe SAC on Mo₂CT₂ (T= O, F, and OH) ^[13]	Micropollutant removal

References

1. J. K. Nørskov, J. Rossmeisl, A. Logadottir, L. Lindqvist, J. R. Kitchin, T. Bligaard and H. Jónsson, *The Journal of Physical Chemistry B*, 2004, **108**, 17886-17892.
2. E. Sargeant, F. Illas, P. Rodríguez and F. Calle-Vallejo, *Journal of Electroanalytical Chemistry*, 2021, **896**, 115178.
3. M. W. Chase, *NIST – JANAF Thermochemical Tables, 4th Edition*, 1998.
4. A. Hjorth Larsen, J. Jørgen Mortensen, J. Blomqvist, I. E. Castelli, R. Christensen, M. Dułak, J. Friis, M. N. Groves, B. Hammer, C. Hargus, E. D. Hermes, P. C. Jennings, P. Bjerre Jensen, J. Kermode, J. R. Kitchin, E. Leonhard Kolsbjerg, J. Kubal, K. Kaasbjerg, S. Lysgaard, J. Bergmann Maronsson, T. Maxson, T. Olsen, L. Pastewka, A. Peterson, C. Rostgaard, J. Schiøtz, O. Schütt, M. Strange, K. S. Thygesen, T. Vegge, L. Vilhelmsen, M. Walter, Z. Zeng and K. W. Jacobsen, *J Phys Condens Matter*, 2017, **29**, 273002.
5. Q. X. Xia, J. Fu, J. M. Yun, R. S. Mane and K. H. Kim, *RSC Advances*, 2017, **7**, 11000-11011.
6. S. Zhou, Y. Zhao, R. Shi, Y. Wang, A. Ashok, F. Héraly, T. Zhang and J. Yuan, *Advanced Materials*, 2022, **34**, 2204388.
7. D. Kan, D. Wang, X. Zhang, R. Lian, J. Xu, G. Chen and Y. Wei, *Journal of Materials Chemistry A*, 2020, **8**, 3097-3108.
8. D. Zhao, Z. Chen, W. Yang, S. Liu, X. Zhang, Y. Yu, W.-C. Cheong, L. Zheng, F. Ren, G. Ying, X. Cao, D. Wang, Q. Peng, G. Wang and C. Chen, *Journal of the American Chemical Society*, 2019, **141**, 4086-4093.
9. J. Zhang, E. Wang, S. Cui, S. Yang, X. Zou and Y. Gong, *Nano Letters*, 2022, **22**, 1398-1405.
10. W. Peng, M. Luo, X. Xu, K. Jiang, M. Peng, D. Chen, T.-S. Chan and Y. Tan, *Advanced Energy Materials*, 2020, **10**, 2001364.
11. Y. Zou, S. A. Kazemi, G. Shi, J. Liu, Y. Yang, N. M. Bedford, K. Fan, Y. Xu, H. Fu, M. Dong, M. Al-Mamun, Y. L. Zhong, H. Yin, Y. Wang, P. Liu and H. Zhao, *EcoMat*, 2023, **5**, e12274.
12. Z. Kou, W. Zang, W. Pei, L. Zheng, S. Zhou, S. Zhang, L. Zhang and J. Wang, *Journal of Materials Chemistry A*, 2020, **8**, 3071-3082.
13. L. Jin, S. You, N. Ren, B. Ding and Y. Liu, *Environmental Science & Technology*, 2022, **56**, 11750-11759.